NANO LETTERS

Letter

Fast, Sensitive Hydrogen Gas Detection Using Single Palladium Nanowires That Resist Fracture

Fan Yang, David K. Taggart, and Reginald M. Penner

Nano Lett., **2009**, 9 (5), 2177-2182• Publication Date (Web): 24 April 2009

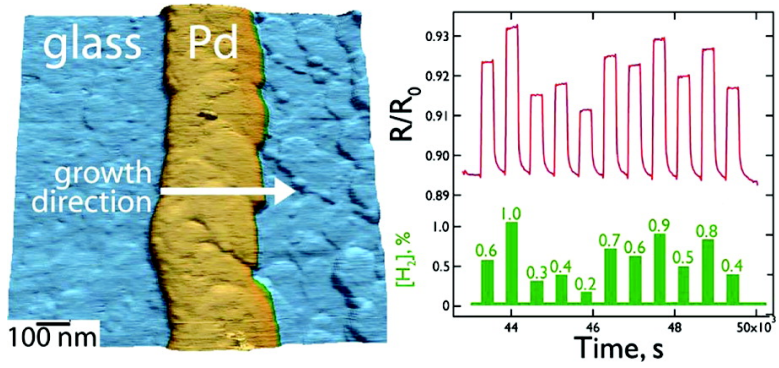

More About This Article

Additional resources and features associated with this article are available within the HTML version:

- Supporting Information
- Access to high resolution figures
- Links to articles and content related to this article
- Copyright permission to reproduce figures and/or text from this article

View the Full Text HTML

NANO LETTERS

2009
Vol. 9, No. 5
2177-2182

Fast, Sensitive Hydrogen Gas Detection Using Single Palladium Nanowires That Resist Fracture

Fan Yang, David K. Taggart, and Reginald M. Penner*

Department of Chemistry, University of California, Irvine, California 92697-2025

Received March 16, 2009; Revised Manuscript Received April 13, 2009

ABSTRACT

Two types of pure palladium (Pd) nanowires, differentiated by microstructure, were electrodeposited: (1) nanocrystalline Pd nanowires (grain diameter ≈ 5 nm, henceforth *nc5*-Pd) and (2) nanocrystalline Pd nanowires with a grain diameter of 15 nm (*nc15*-Pd). These nanowires were evaluated for the detection of hydrogen gas (H_2). Despite their fundamental similarities, the behavior of these nanowires upon exposure to H_2 was dramatically and reproducibly different: *nc5*-Pd nanowires spontaneously fractured upon exposure to H_2 above 1−2%. Fractured nanowires continued to function as sensors for H_2 concentrations above 2%, actuated by the volume change associated with the α to β phase transition of PdH_x. *nc15*-Pd nanowires, in contrast, withstood repeated exposures to H_2 up to 10% without fracturing. *nc15*-Pd nanowires showed a rapid (2 s at 10%) increase in resistance in the presence of H_2 and a response that scaled smoothly with [H_2] spanning 5 orders of magnitude down to 2 ppm.

Hydrogen (H_2) gas sensors that are sensitive, rapid-responding, stable, compact, and inexpensive are needed to optimize the performance and ensure the safety of devices like fuel cells that are powered by H_2. Palladium (Pd) nanowires are attractive candidates for H_2 sensors because they are able to equilibrate rapidly with H_2, leading to a rapid response time. Palladium absorbs hydrogen to form a hydride (PdH_x) with x saturating at 0.67,[1,2] and since 1869 it has been known that the electrical resistivity of this hydride increases linearly with x by a factor of 1.8−1.9 over the range from $x = 0$ to 0.67.[1] This property of PdH_x was first exploited for hydrogen sensing by Hughes and Schubert 1992.[3] As hydrogen gas sensors, Pd resistors are elegant in their simplicity but they have several deficiencies: (1) Hydrogen atom diffusion in palladium is slow at room temperature ($D_H = 3.8 \times 10^{-7}$ cm^2/s at 298 K).[1,2] This means that the Pd resistor must be heated to 70 °C or higher to activate diffusion degrading the power efficiency of the device. (2) The α to β phase transition of PdH_x, occurring over the range from 1 to 2% H_2 (in this paper we refer exclusively to the volumetric percentage, v/v %), mechanically stresses the resistor causing deformation and delamination while simultaneously retarding the sensor response time. (3) hydrogen sulfide, ammonia, water, and hydrocarbons interfere with H_2 detection at Pd because they dissociatively chemisorb, often irreversibly, to produce adsorbed hydrogen atoms and block the adsorption of dihydrogen.

By reducing the distance over which hydrogen must diffuse within the palladium sensing element, the retarding effect of slow proton diffusion on the response time of the resistor is minimized. This was the rational for exploring the use of palladium nanowires in hydrogen sensors in 2001.[4] These early sensors[4,5] consisted of ensembles of hundreds of Pd nanowires, 150−300 nm in diameter. Exposure of these nanowires to H_2 at concentrations above 2% caused each nanowire to fracture approximately every 2 μm along its axis resulting in a loss of electrical continuity. Subsequent exposures to H_2 above the 1−2% threshold for the α to β phase transition swelled the nanowire and closed these fractures, restoring electrical continuity. These sensors had a rapid response time of <1 s, but the limit-of-detection (LOD_{H_2}) was in the 2% range necessary to induce the α to β phase transition. This LOD_{H_2} is too high even for H_2 leak detection since the lower explosion limit for H_2 of 4% is just incrementally higher.

Since 2002, palladium nanostructures have been used in a variety of innovative ways as resistor-based hydrogen sensors. These sensors can be categorized according to the mechanism by which they transduce hydrogen: Sensors that derive their signal from the volume change associated with the α to β phase transition generally show decreased resistance in the presence of hydrogen (i.e., $\Delta R_{H_2}(-)$) while those that measure the increased resistance of the PdH_x relative to Pd show an increased resistance upon H_2 exposure (i.e., $\Delta R_{H_2}(+)$). Two-dimensional palladium nanoparticulate films[6−11] fall into the first category. An attribute of these systems is that they often have rapid response times (<1s) that mimic the early palladium nanowire arrays,[4,5] and they

10.1021/nl9008474 CCC: $40.75
Published on Web 04/24/2009

are much easier to fabricate. Yun and co-workers[12] electrodeposited single palladium nanowires and showed that these function as H_2 sensors in this $\Delta R_{H_2}(-)$ mode. A $\Delta R_{H_2}(-)$ sensor was also produced by using a focused ion beam to cut a nanotrench with width 100−400 nm into a palladium microwire.[13] With a few exceptions,[8,14] $\Delta R_{H_2}(-)$ sensors show a LOD_{H_2} in the 1−2% range coinciding with the threshold for the α to β phase transition. A lower LOD_{H_2} can be obtained for systems capable of functioning in the $\Delta R_{H_2}(+)$ regime because the increased resistance of PdH_x can be detected well below the 1−2% threshold for the α to β phase transition, often at the expense of slower sensor response and recovery times. Myung and co-workers[15] recently showed that a sensitive $\Delta R_{H_2}(+)$ hydrogen sensor is obtained when carbon nanotubes arrayed between two electrical contacts are electrochemically decorated with palladium nanoparticles. These sensors showed a LOD_{H_2} of 100 ppm with response times in the 5−10 min range. We demonstrate below that by controlling the grain structure of a palladium nanowire, nanowires operating in either the $\Delta R_{H_2}(+)$ or the $\Delta R_{H_2}(-)$ modes can be obtained. But superior H_2 sensing performance, including response times in the 1−5 s range at high H_2 concentrations and a LOD_{H_2} of 2 ppm, are demonstrated for single Pd nanowire sensors operating in the $\Delta R_{H_2}(+)$ mode that did not break upon exposure to H_2.

The Pd nanowires used in this study were prepared using lithographically patterned nanowire electrodeposition (LPNE).[16,17] *nc5*-Pd nanowires were prepared by electrodepositing Pd at a potential of +0.18 V vs saturated calomel electrode (SCE) from an aqueous electrolyte (0.2 mM $PdCl_2$, 0.1 M KCl, pH = 4.9) at current densities approximately 1 order of magnitude below diffusion control. *nc15*-Pd nanowires were electrodeposited at a potential of −0.80 V vs SCE from the same aqueous electrolyte except for the addition of 0.22 mM EDTA (ethylenediaminetetraacetic acid). The complexation of palladium ion by EDTA caused a negative shift in the threshold for Pd deposition, but the deposition potential more than compensated for this shift, producing a deposition rate that was an order of magnitude larger than that used in the EDTA-free Pd depositions.

LPNE produces nanowires that have a rectangular cross section with a well-defined height and width that are independently adjustable over a wide range. In this study we probed nanowires ranging in height from 11 to 48 nm and in width from 36 to 93 nm. An array of palladium nanowires produced by LPNE is shown in the atomic force microscope (AFM) images of Figure 1. The AFM images of nanowires deposited from EDTA-free and EDTA-containing solutions were identical, but important morphological differences between them are readily apparent in transmission electron micrographs (Figure 1c,d) which were acquired at nine tilt angles (−8° to +8° at 2° increments) in order to facilitate the identification of individual grains. In these bright-field images, individual Pd grains become dark when their crystallographic orientation meets the condition for diffracting the electron beam, deflecting it off the detector. The grain size distribution is obtained by measuring these

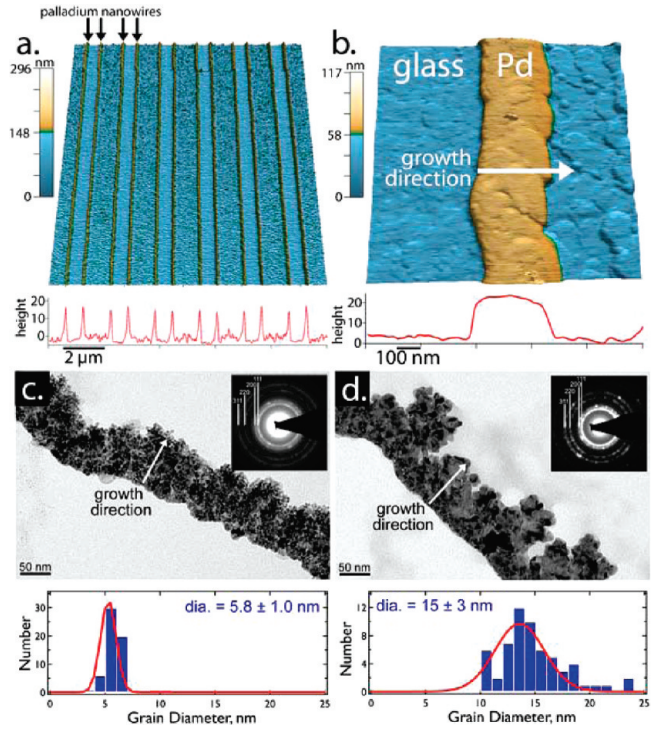

Figure 1. Pd nanowires prepared by LPNE: (a, b) atomic force microscope images of Pd nanowires at low (a) and high (b) magnification; (c, d) TEM images of Pd nanowires prepared in the absence of EDTA (c) and presence of EDTA (d) showing the grain structure. Grain diameter histograms for wires of each type are also shown.

darkened grains in a series of tilted images, and it should be understood that this transmission electron microscopy (TEM) analysis probes only the in-plane grain dimension. Just one TEM image from each series is shown in Figure 1c,d, together with the grain diameter histograms assembled from these two tilt series. These images show that Pd nanowires deposited from the EDTA-free solution (henceforth, *nc5*-Pd) are nanocrystalline with a narrow grain diameter distribution peaking at 5.8 nm. In the micrograph of Figure 1c, the 5−6 nm grains are all approximately round and the wire morphology is quite open, with cracks and voids apparent between grains, especially at wire edges. The effect of added EDTA on the microstructure of electrodeposited metals has not been explored to our knowledge. We found that palladium nanowires deposited in the EDTA-containing electrolyte (*nc15*-Pd nanowires) had a larger mean grain diameter of 15 nm and a broader distribution of grain diameters. *nc15*-Pd nanowires also have a more compact, electron dense morphology despite the fact that both nanowires shown here had the same total thickness of 20 nm. It is possible that carbon incorporation occurs for the *nc15*-Pd nanowires deposited from the EDTA-containing solution, but carbon was not detected above background in EDAX (X-ray fluorescence) elemental analyses of these nanowires. Thus, both the *nc5*-Pd and *nc15*-Pd nanowires are nanocrystalline, but as we discuss next, the subtle morphological differences seen in Figure 1c,d translate into dramatic differences in their hydrogen-sensing performance.

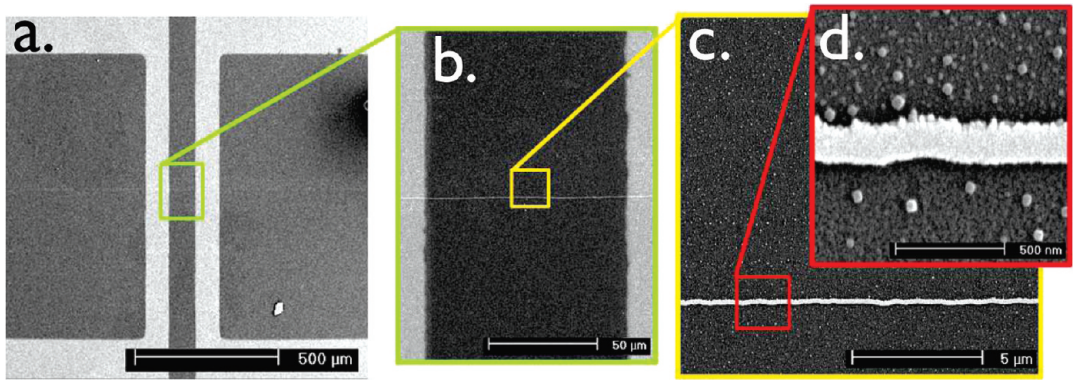

Figure 2. Pd nanowire-based H_2 sensors. (a−c) Scanning electron microscope images at progressively higher magnification of a H_2 sensor consisting of a single Pd nanowire with evaporated four-contact electrodes.

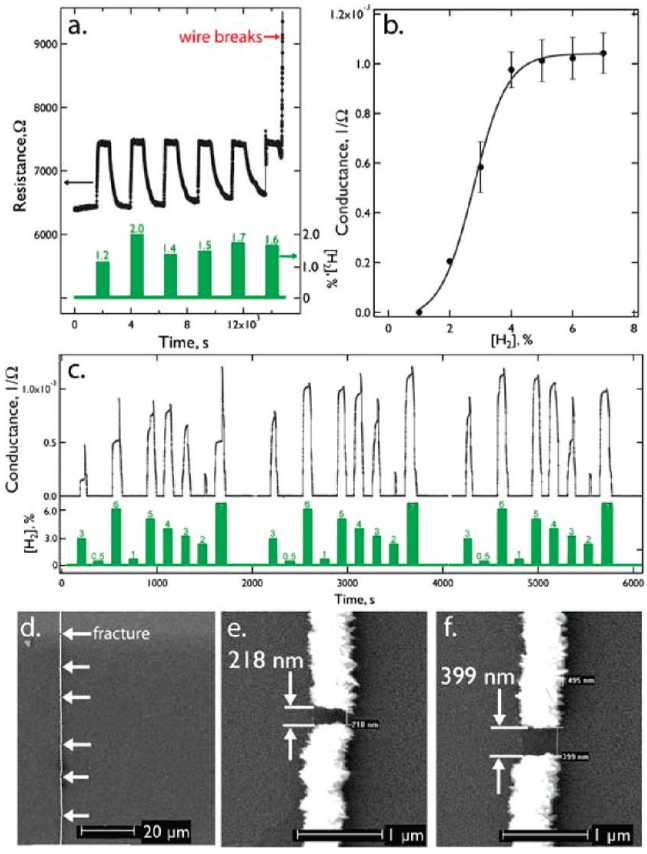

Figure 3. Fracture of *nc5*-Pd nanowire upon H_2 exposure. (a) Plots of resistance versus time during the exposure of a single 40 × 430 nm Pd nanowire to pulses of 1.2%−2.0% hydrogen as indicated by the program at bottom. Fracture of the nanowire on the sixth exposure is signaled by an increase in the resistance to >10 M Ω. (b) Calibration plot for the response of a fractured *nc5*-Pd nanowire to H_2. Error bars indicate ±1 standard deviation of the mean for multiple trials. (c) Conductance versus time for the exposure of a fractured *nc5*-Pd nanowire to pulses of hydrogen ranging in concentration from 0.5% to 7% (d−f) Scanning electron microscope images at low magnification (d) and higher magnification (e, f) showing fractures produced by H_2 exposure.

From a purely electrical standpoint, *nc15*-Pd nanowires and *nc5*-Pd nanowires were similar: *nc15*-Pd nanowires electrodeposited from EDTA-containing solutions had electrical resistivities that were ≈30% lower than those obtained

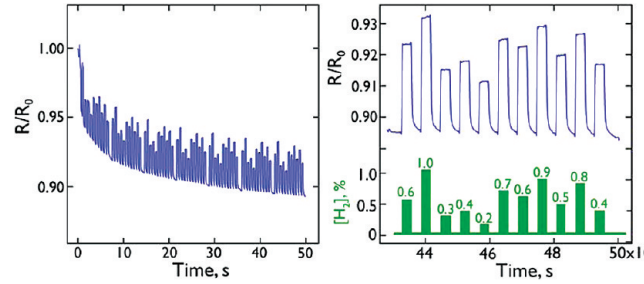

Figure 4. Initial exposures of a 20 × 42 nm *nc15*-Pd nanowire to H_2. (a) R/R_0 versus time for the exposure to 77 pulses of H_2 ranging in concentration from 0.2% to 1.0%. (b) R/R_0 versus time for the final sequence of 11 H_2 exposures comparing the applied concentration program (bottom) with the observed nanowire response (top).

for *nc5*-Pd nanowires of closely matched height and width—qualitatively as expected and as reported previously for other metals, such as copper.[18,19] These resistance values are 20−50 times higher than those for bulk palladium.[17]

Hydrogen sensors were fabricated from single Pd nanowires supported on glass by evaporating gold electrical contacts (Figure 2a) and attaching copper wires to these contacts using silver paint. These evaporated contacts isolated a 100 μm length of each nanowire (Figure 2b) and the electrical resistance of this wire section was measured using four electrical contacts as a function of time during the exposure of the sensor to pulses of hydrogen of predetermined concentration—determined by mixing of H_2 and N_2 flow streams at flow rates determined by mass flow controllers—in a flowing stream of pure nitrogen gas.

A plot of resistance versus time for the exposure of a single *nc5*-Pd nanowire to a series of hydrogen pulses near 1% is shown in Figure 3a. An increase in the wire resistance ($\Delta R/R_0 \approx 15\%$) is seen during each hydrogen exposure for the first five of these pulses and then, during the sixth pulse, the resistance increases to more than 10 MΩ. This rapid increase in resistance signals the formation of fractures in the Pd nanowire. After fracturing, the *nc5*-Pd nanowire shows no detectible response to H_2 exposure below 1%, but for higher concentrations, the nanowire resistance rapidly and reversibly decreases and the amplitude of this resistance change, plotted as an increased conductance in Figure 3c, correlates with

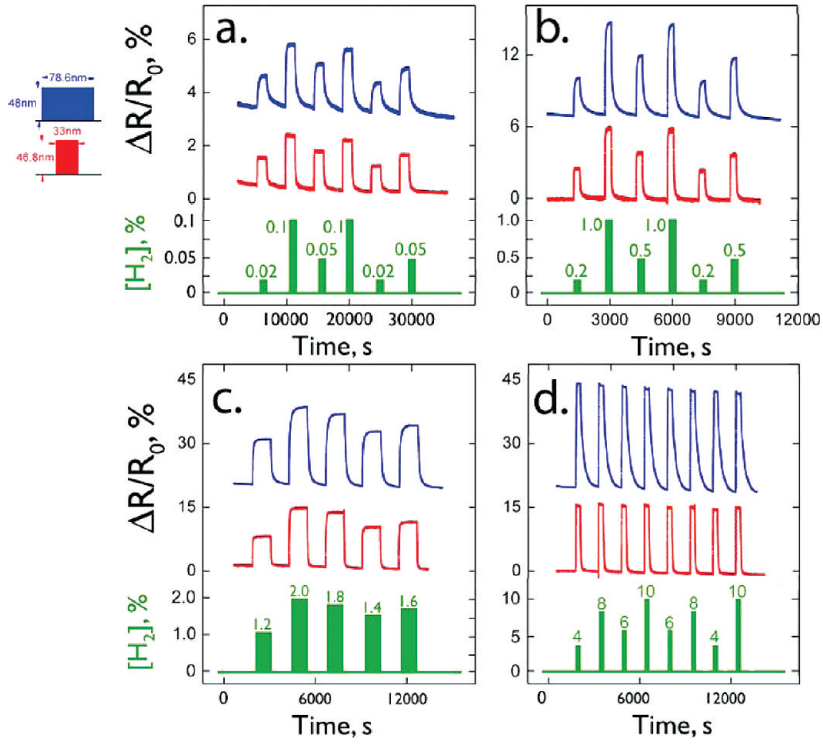

Figure 5. $\Delta R/R_0$ response of two *nc15*-Pd nanowire sensors (inset) over a wide $[H_2]$ range. (a) 0.02% to 0.1% pulses with a duration of 9 h, (b) 0.2% to 1.0% H_2 pulses with a duration of 3 h, (c) 1.2% to 2.0% H_2 pulses with a duration of 3.5 h, and (d) 4% to 10% H_2 with a duration of 3.5 h.

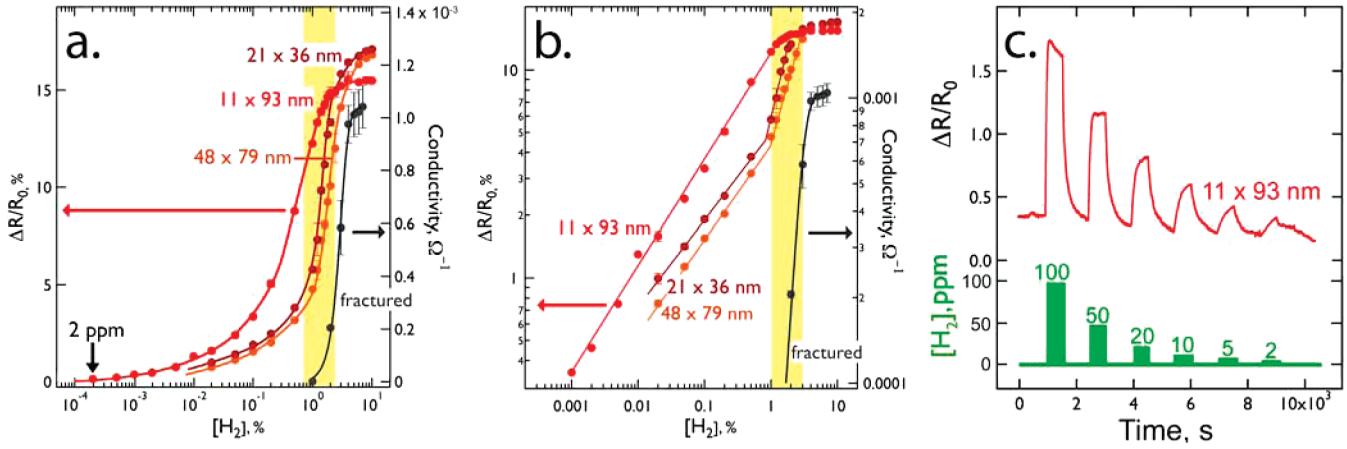

Figure 6. Calibration curves for three *nc15*-Pd nanowires and a fractured *nc5*-Pd nanowire. (a) $\Delta R/R_0$ (or conductivity) versus log$[H_2]$ response. (b) log−log representation of the same data shown in (a). (c) Response of the 11 × 93 nm *nc15*-Pd nanowire to $[H_2]$ from 2 to 100 ppm.

the $[H_2]$ over a narrow concentration range from 1 to 5%. For $[H_2]$ above 5%, no change in conductance is seen over that measured at 5%. Over this 1−5% range, the reproducibility of the conductance change is 10−20% (Figure 3b). These response characteristics are, in all respects, similar to those reported for other $\Delta R_{H_2}(-)$ sensors that transduce H_2 using the α to β phase transition of PdH_x.[4−11,13]

That fracturing of the *nc5*-Pd nanowires has occurred is confirmed by SEM examination of *nc5*-Pd nanowire after exposure to H_2 (Figure 3d). These nanowires are fractured periodically, every 10 μm, along the nanowire length with each fracture defined by a 200−400 nm gap. The integrated gap length along each fractured nanowire corresponds to 3−4%, approaching the expected 3.5% linear expansion induced by the α to β phase transition of PdH_x.[1] Previously,[4,5] we studied the properties of ensembles of 200 nm diameter Pd nanowires for sensing hydrogen and we observed exactly the same fracturing behavior in response to hydrogen exposure for these much larger nanowires. In 13 trials involving the exposure of *nc5*-Pd nanowires to hydrogen in the concentration range near 1%, all 13 nanowire fractured in the manner depicted in Figure 3. We conclude that the sensing mechanism for fractured *nc5*-Pd nanowires involves the mechanical closing of these fractures upon exposure to H_2 above 1% caused by the α to β phase transition of PdH_x and the simultaneous swelling by 3.5% of the PdH_x wire's

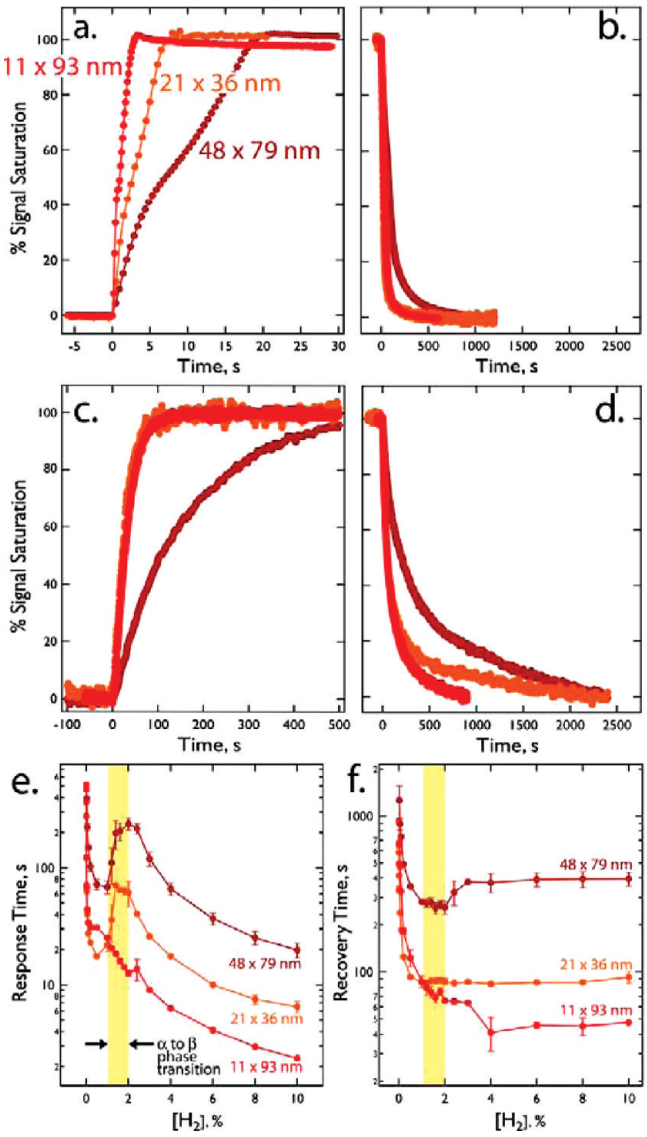

Figure 7. Comparison of temporal response characteristics for three *nc15*-Pd nanowires: (a) response to $H_2 = 10\%$, (b) recovery from exposure to $H_2 = 10\%$, (c) response to $H_2 = 0.02\%$, (d) recovery from exposure to $H_2 = 0.02\%$, (e) summary of response times as a function of $[H_2]$ for three *nc15*-Pd nanowires, and (f) summary of recovery times as a function of $[H_2]$ for the same three nanowires.

linear dimensions relative to Pd. A suspended wire in tension should fracture once, not multiple times, so the existence of multiple fractures (also as seen previously)[4,5] requires multiple strong points of attachment between the wire and the glass surface—a minimum of one per fracture—arrayed along each nanowire.

nc15-Pd nanowires did not fracture upon exposure to hydrogen at any concentration, and this fact permits these nanowires to operate in the $\Delta R_{H_2}(+)$ mode, enabling far superior H_2 sensing performance as compared with *nc5*-Pd nanowires. The resistance of a freshly prepared *nc15*-Pd nanowire is shown in Figure 4a as it is repeatedly exposed to a sequence of H_2 pulses ranging in concentration from 0.2 to 1.0% over 14 h. Significant drift of the baseline resistance is seen in these data, but the drift decreases progressively over the 14 h experiment until at its conclusion, it is reduced to $\Delta R/R_0 \approx 0.09\%$/hour. We preconditioned each *nc15*-Pd nanowire employed for sensing to stabilize its baseline resistance using this procedure.

Raw sensing data for two different *nc15*-Pd nanowires (Figure 5) show rapid, reversible increases in resistance for $[H_2]$ ranging from 0.02% to 10%. But the signal-to-noise seen in Figure 5a at the lower end of this range supports the detection of much lower H_2, down to 2 ppm (Figure 6c). Calibration plots for nanowires of different widths and heights (Figure 6a,b) show very clearly the extended concentration range over which the *nc15*-Pd nanowires are able to operate relative to the *nc5*-Pd nanowires (labeled "fractured"). Less obvious, but of equal importance, is a tremendous improvement in the reproducibility of the $\Delta R/R_0$ seen at each concentration which is reflected by the error bars in each data set. These calibration plots also reveal that $\Delta R/R_0$ is insensitive to the cross-sectional wire dimensions, and its initial resistance, to first order. For example, the electrical resistance of the smaller nanowire (21 × 36 nm) was 305 kΩ and that of the larger nanowire (48 × 79 nm) was 40.8 kΩ, but these two nanowires produced the same $\Delta R/R_0$, to within 5% over the entire concentration range from $[H_2] = 0.02$ to 10%.

The response and recovery times for *nc15*-Pd nanowires, on the other hand, were strongly dependent on the wire cross-sectional dimensions (Figure 7). We define these two metrics here as the time necessary for the $\Delta R/R_0$ to achieve 90% of their respective values at infinite time. Two features of the data shown in Figure 7 are worth noting: First, above $[H_2] = 1\%$, response and recovery times decrease by approximately an order of magnitude as the wire height is reduced from 48 to 21 nm to 11 nm despite the fact that the wire width does not change monotonically for these three wires. Thus, the wire height is the main predictor of the temporal response and recovery times for *nc15*-Pd nanowires. For lower $[H_2]$, the effect of wire size is still present but somewhat weaker. Second, the response time for the nanowires with $(h) = 21$ and 48 nm is retarded in the concentration range from 1 to 2%. This concentration range coincides with the α to β phase transition, and it is likely that this phase transition is the origin for the slowed sensor response seen here (Figure 7e). We hypothesize that the retarding influence of the phase transition on sensor response is most prevalent at 1−2% and less prevalent at higher concentrations, because the phase transition itself is first order in dihydrogen, and so it is accelerated at higher hydrogen concentrations whereas at lower hydrogen concentrations, below 1%, it does not occur at all. The existence of this peak strongly suggests the α to β phase transition prevents nanowires from rapidly equilibrating with the hydrogen concentration, particularly at the $[H_2] = 1-2\%$ threshold for the phase transition. This slowing of the sensor response depends strongly on the cross-sectional dimensions of the nanowires and it is not observed at all for the smallest nanowire we examined, with $(h) = 11$ nm. The implication is that smaller nanowires are able to more rapidly accommodate the strain imposed by the ≈10% volume change associated with this phase transition.

The origin of the disparate mechanical behavior of the *nc5*-Pd nanowires and the *nc15*-Pd nanowires we have examined here is not addressed by our data. The canonical behavior for polycrystalline metals is increasing yield-strength, σ_y, with a reduction in the grain diameter, d, according to the Hall−Petch equation[20,21]

$$\sigma_y = \sigma_0 + \frac{k_y}{\sqrt{d}} \quad (1)$$

where σ_0 is a materials constant for the starting stress for dislocation movement and k_y is the strengthening coefficient. In the sub-100-nm grain size regime that applies in this study, *inverse* Hall−Petch behavior characterized by weakening yield strength with reduction of the grain size has also been reported.[22] To date there have been no investigations of the tensile stress−strain behavior of polycrystalline nanowires to our knowledge, but these data highlight the importance of these investigations, and we are working to carry them out in our laboratory.

In summary, the effect of grain structure on the functional properties of polycrystalline nanowires has not been examined in any context, to our knowledge. Here we have demonstrated that for nanowires of pure palladium a subtle difference in grain structure is associated with disparate wire behavior upon exposure to hydrogen gas leading to radically altered functionality in the application of these nanowires as hydrogen sensors. Specifically, single *nc15*-Pd nanowires prepared from EDTA-containing plating solution are not subject to fracturing when exposed to hydrogen and, for this reason, they are able to rapidly and reversibly detect hydrogen as a resistance increase down to 2 ppm with excellent reproducibility and baseline stability at room temperature.

Acknowledgment. This work was supported by National Science Foundation Grant CHE-0641169, the Petroleum Research Fund of the American Chemical Society 46815-AC 10, and the UCI School of Physical Sciences Center for Solar Energy.

References

(1) Lewis, F. A. *The palladium hydrogen system*; Academic Press: London, 1967.
(2) Flanagan, T. B.; Oates, W. A. *The palladium-hydrogen system*; Annual Reviews, Inc.: Palo Alto, CA1991; Vol. 21, pp 269−304.
(3) Hughes, R. C.; Schubert, W. K. *J. Appl. Phys.* **1992**, *71*, 542–544.
(4) Favier, F.; Walter, E.; Zach, M.; Benter, T.; Penner, R. *Science* **2001**, *293*, 2227–2231.
(5) Walter, E.; Favier, F.; Penner, R. *Anal. Chem.* **2002**, *74*, 1546–1553.
(6) Dankert, O.; Pundt, A. *Appl. Phys. Lett.* **2002**, *81*, 1618–1620.
(7) Kaltenpoth, G.; Schnabel, P.; Menke, E.; Walter, E.; Grunze, M.; Penner, R. *Anal. Chem.* **2003**, *75*, 4756–4765.
(8) Xu, T.; Zach, M.; Xiao, Z.; Rosenmann, D.; Welp, U.; Kwok, W.; Crabtree, G. *Appl. Phys. Lett.* **2005**, *86*, 203104.
(9) Luongo, K.; Sine, A.; Bhansali, S. *Sens. Actuators, B* **2005**, *111*, 125–129.
(10) Khanuja, M.; Varandani, D.; Mehta, B. R. *Appl. Phys. Lett.* **2007**, *91*, 253121.
(11) Ibanez, F. J.; Zamborini, F. P. *J. Am. Chem. Soc.* **2008**, *130*, 622–633.
(12) Im, Y.; Lee, C.; Vasquez, R.; Bangar, M.; Myung, N.; Menke, E.; Penner, R.; Yun, M. *Small* **2006**, *2*, 356–358.
(13) Kiefer, T.; Favier, F.; Vazquez-Mena, O.; Villanueva, G.; Brugger, J. *Nanotechnology* **2008**, *19*, 125502.
(14) Kim, K.; Sim, S.; Cho, S. *IEEE Sens. J.* **2006**, *6*, 509–513.
(15) Mubeen, S.; Zhang, T.; Yoo, B.; Deshusses, M. A.; Myung, N. V. *J. Phys. Chem. C* **2007**, *111*, 6321–6327.
(16) Menke, E. J.; Thompson, M. A.; Xiang, C.; Yang, L. C.; Penner, R. M. *Nat. Mater.* **2006**, *5*, 914–919.
(17) Xiang, C.; Kung, S. C.; Taggart, D.; Yang, F.; Thompson, M. A.; Güell, A. G.; Yang, Y.; Penner, R. M. *ACS Nano* **2008**, *2*, 1939–1949.
(18) Steinhogl, W.; Schindler, G.; Steinlesberger, G.; Engelhardt, M. *Phys. Rev. B* **2002**, *66*, 075414.
(19) Steinhogl, W.; Schindler, G.; Steinlesberger, G.; Traving, M.; Engelhardt, M. *J. Appl. Phys.* **2005**, *97*, 023706.
(20) Petch, N. *J. Iron Steel Inst., London* **1953**, 25–28.
(21) Hall, E. *Phys. Soc., Ser. B* **1951**, *64*, 747–753.
(22) Carlton, C. E.; Ferreira, P. J. *Acta Mater.* **2007**, *55*, 3749–3756.

NL9008474